PHYSICAL REVIEW B VOLUME 58, NUMBER 16 15 OCTOBER 1998-II

Molecular orientation determined by second-harmonic generation: Self-assembled monolayers

Frank Eisert, Oliver Dannenberger,* and Manfred Buck
Lehrstuhl für Angewandte Physikalische Chemie, INF 253, 69120 Heidelberg, Germany

(Received 20 January 1998)

Monolayers of 12-(4-nitroanilino)-dodecane thiol $[O_2N-C_6H_4-NH(CH_2)_{12}SH]$(NAT) adsorbed on polycrystalline gold substrates were investigated in a gaseous environment and in ethanol. Contributions of comparable magnitude from the metal substrate, the adsorbate-substrate interaction, and the *p*-nitro aniline moiety (*p*NA) require phase-sensitive and polarization-dependent second-harmonic-generation (SHG) measurements. The susceptibility of the *p*NA end group is separated by comparative experiments with *n*-alkane thiols. Evaluation of the orientation of the *p*NA moiety requires phase information about the SHG signal. Intensity data alone produce ambiguous results. The tilt angle determined by SHG is shown to be strongly dependent on the model applied. For the NAT film in an inert gas atmosphere, the tilt angle ϑ of the *p*NA group calculated from the SHG experiments is compared with the value of 53° obtained by linear techniques. Agreement is only achieved if local-field factors are neglected and if a two-layer model is assumed to describe the linear optical properties of the system. Immersion of the NAT film in ethanol causes a change of the tilt angle of the *p*NA end group to a more upright position of about $\vartheta=36°$. A detailed discussion reveals that the accuracy and reliability of SHG data to determine the orientation of molecules depend critically on the precision by which molecular properties are known and on the model describing the linear optical properties.
[S0163-1829(98)11339-5]

I. INTRODUCTION

For the investigation of processes and properties related to ultrathin organic films,[1] a wealth of particle-based techniques is available. However, different techniques are required for the investigation of, e.g., processes at electrode surfaces or wetting phenomena. Among these, photon-based methods play a crucial role. Besides linear optical techniques such as ellipsometry, surface plasmon resonance, IR spectroscopy, or surface-enhanced Raman spectroscopy,[1] nonlinear optical methods (nlo), i.e., second-harmonic generation (SHG) and sum frequency generation (SFG), have been successfully applied to problems related to molecular layers[2–10]. The combination of an intrinsic interface sensitivity, high versatility with respect to the choice of the environment, submolecular resolution by selectively addressing bonds or submolecular units, and the possibility to determine molecular orientation by polarization-dependent measurements, make SHG and SFG appealing to tackle problems related to molecular layers. However, the advantages of these techniques are contrasted by certain restrictions. One is a sufficiently high nlo activity which in the case of SHG usually requires an aromatic system.[11] Another one is that the hyperpolarizability tensor has to be simple and well known to allow a straightforward interpretation of the experimental data. In addition, the results are substantially affected by other factors such as the effective electric fields acting on a molecule and the linear optical properties of the system. A survey of the literature reveals a very diverse picture. Local-field corrections are either taken into account[12–15] or not[16,17] for the determination of molecular orientation in organic films. Furthermore, the optical properties of adsorbate/substrate systems are sometimes described by three layers, i.e., an index of refraction is assigned to the molecular layer,[13,14,16,18–20] sometimes by two layers with the optical constants of the film identified with the surrounding media.[21,22] At present no conclusive picture exists which apply to the model. A problem is that the experimental data usually yield a result regardless of the details of the model. A molecular orientation easily can be obtained by polarization-dependent SHG measurements. However, the crucial question is the following: How does the calculated tilt angle depend on the model and, thus, what is the meaning of the value? Zhang, Zhang, and Wong already demonstrated that the results are sensitively dependent on the model.[23] In order to address this question in more detail, investigations are required which compare results from nonlinear techniques with those obtained by independent methods. Unfortunately, this has not been done so far.

The work presented below is a SHG study on a model system for which such a comparison is possible. 12-(4-nitroanilino)-dodecane thiol $[O_2N-C_6H_4-NH(CH_2)_{12}SH]$ (NAT) adsorbed on gold substrates has been investigated previously by IR-reflection-absorption spectroscopy (IRRAS) and near-edge x-ray-absorption fine-structure spectroscopy (NEXAFS).[24] NAT, which consists of an alkane thiol terminated by a *p*-nitroaniline (*p*NA) end group, belongs to the class of self-assembling monolayers (SAM's) which have recently become a focus of interest due to their application potential in a variety of fields, e.g., (bio)sensorics, electrochemistry, or lithography.[1,25–31] For part of the applications the properties of SAM's under nonvacuum conditions, e.g., in contact to liquids, has to be known. Thus, an investigation of the environment-dependent behavior of the molecules, i.e., orientation and conformation, is an important aspect, and is the motivation to apply *in situ* techniques such as SHG. At the same time this issue relates to the crucial question to what extend information about SAM's obtained in gaseous or even ultrahigh-vacuum environment can be transferred to condensed media.

The *p*NA moiety was chosen since, with respect to SHG

0163-1829/98/58(16)/10860(11)/$15.00

studies, it is one of the best studied systems, and thus its nlo properties have been thoroughly studied both theoretically and experimentally.[11] NAT on a gold substrate represents an extension of SHG work on molecular films. Usually, SHG active molecules on SHG inactive substrates are investigated or in the case where the substrate is metallic both the substrate signal and the adsorbate-substrate interaction are weak and thus the adsorbate signal dominates.[8,22,32,33] The present case is the most general in the sense that all three contributions—from the substrate, from the adsorbate-substrate interaction, and from the adsorbate—are non-negligible, and, therefore, the molecular contribution has to be separated. Furthermore, the metallic substrate causes the different contributions to be phase shifted against each other. This makes phase-sensitive detection mandatory.

II. THEORY

A. Separation of contributions

Based on the electric dipole approximation the intensity of the second harmonic signal I_{SHG} is given by[8,10]

$$I_{SHG}=A|e^{2\omega}\chi_{tot}^{eff}e^{\omega}e^{\omega}|^2 I_{\omega}^2, \qquad (1)$$

where I_{ω} is the intensity of the incident radiation at the fundamental frequency, and A is an experiment-dependent constant[8]. The third rank tensor χ_{tot}^{eff} denotes an effective second-order susceptibility. $e^{2\omega}$ and e^{ω} are the unit polarization vectors. For an adsorbate/substrate system of the type investigated here (Fig. 1), the SHG signal is a coherent superposition of three different sources, and χ_{tot}^{eff} can be written as

$$\chi_{tot}^{eff}(\lambda,\theta)=\chi_{sub}^{eff}(\lambda)+\chi_{int}^{eff}(\lambda,\theta)+\chi_{ads}^{eff}(\lambda,\theta). \qquad (2)$$

χ_{sub} represents the second-order optical properties of the bare gold substrate, χ_{int} reflects its alteration by the interaction with the thiol molecules, i.e., the Au-S bond formation, and χ_{ads} represents the nl activity of the molecule.[6,32] The dependence of the susceptibilities from the wavelength λ and the coverage θ (Refs. 5,10, and 34) is explicitly stated in Eq. (2), but will be omitted for simplicity below. In general, the susceptibilities are complex quantities expressed conveniently by the experimentally accessible quantities magnitude $|\chi|$ and phase factor $e^{i\phi}$. Their representation in polar coordinates is illustrated by Fig. 1, with the phase of the substrate susceptibility ϕ_{sub} defined to zero. In the definition of the polar diagram, a counterclockwise rotation of the arrow corresponds to positive phase shifts.

The experimentally accessible quantities about an adsorbate/substrate system are the magnitudes $|\chi_{sub}|$, $|\chi_{tot}|$, and ϕ_{tot}. Therefore, the sum of χ_{int} and χ_{ads} can be determined, only. However, for all SHG studies of adsorbates reported so far either χ_{int} or χ_{ads} are negligible,[8] and thus the measured SH signal directly reflects a particular aspect of the adsorbate such as the molecular orientation or its interaction with the substrate via χ_{ads} or χ_{int}, respectively. In contrast, for a nlo active thiol molecule adsorbed on a metal substrate, all terms of Eq. (2) are comparable in magnitude and thus χ_{int} and χ_{sub} cannot be neglected, even for resonant excitation of the pNA end group. Thus, for the separation of χ_{ads}, two sets of experiments are required: Measurement of NAT on gold and a comparative measurement using unsubstituted n-alkane thiols. For pure hydrocarbon chains the third term of Eq. (2) does not contribute measureably due to the vanishingly low hyperpolarisability of σ bonds.[11] Comparison of films of both thiols at equal coverage thus allows one to separate the susceptibility of the pNA moiety according to

$$\chi_{pNA}=\chi_{tot}^{NAT}-\chi_{tot}^{MC}. \qquad (3)$$

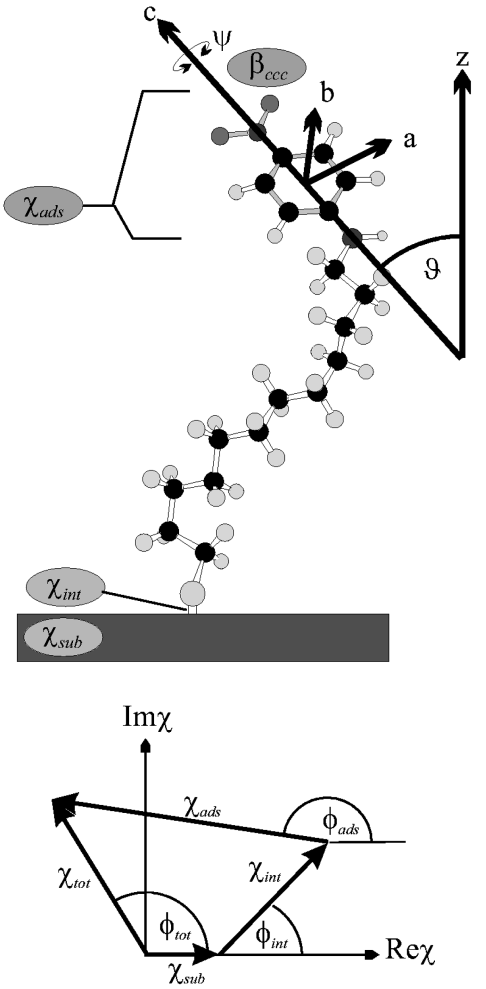

FIG. 1. Schematic illustration of 12-(4-nitroanilino)-dodecane thiol (NAT) adsorbed on gold. The susceptibilities contributing to the second-harmonic signal are indicated, and their superposition in the complex plane according to Eq. (2) is depicted in the vector diagram.

Since the susceptibilities representing the different sources of χ_{tot} are third-rank tensors, the SH signal is a coherent superposition of contributions from different tensor elements.[34] The exact number of contributing elements is determined by the system and the experimental setup. In the present case the number of tensor elements of each source, i.e., substrate, thiol-Au interaction, and pNA moiety, reduces from the most general case of 18 independent elements to only three due to the azimuthal isotropy of the system.[8] The azimuthal isotropy of clean and thiol-covered polycrystalline gold substrates has been checked in a series of independent experiments with the respective samples mounted on a rotation stage.[35] Furthermore, polarization-dependent SHG measurements allow one to separate different tensor elements. For the determination of the orientation of the pNA end group discussed below two polarization combinations of the incident fundamental radiation and the detected SHG signal are relevant: $s_\omega p_{2\omega}$ and $p_\omega p_{2\omega}$ polarizations with s and p defining the polarizations perpendicular and parallel to the plane of incidence. The relations between the experimentally accessible quantities I and ϕ and the nonvanishing elements of the tensor are thus[8,34]

$$\sqrt{I^{sp}_{SHG}}e^{i\phi^{sp}}=A^{1/2}e_z^{2\omega}F_{zyy}\chi_{zxx}e_y^\omega e_y^\omega E_\omega^2 \tag{4}$$

for sp polarization with the identity $\chi_{zxx}=\chi_{zyy}$, and

$$\sqrt{I^{pp}_{SHG}}e^{i\phi^{pp}}=A^{1/2}(e_z^{2\omega}F_{zzz}\chi_{zzz}e_z^\omega e_z^\omega+e_z^{2\omega}F_{zxx}\chi_{zxx}e_x^\omega e_x^\omega$$
$$+2e_x^{2\omega}F_{xzx}\chi_{xzx}e_z^\omega e_x^\omega)E_\omega^2 \tag{5}$$

for pp polarization. x,y,z denote the axes of a Cartesian coordinate system with z parallel to the surface normal. The F_{ijk}'s take into account the modification of the electric fields E_ω due to the interface and additional corrections due to the presence of a highly polarizable monolayer. This will be detailed below.

B. Analysis of molecular orientation

For the molecular orientation to be quantified, the hyperpolarizability tensor of the molecule has to be transformed into a tensor of surface coordinates. The orientation of a nlo moiety is determined most simply if its hyperpolarizability tensor β has a single non-vanishing element.[8,10] To a first approximation this case is met for pNA with the nonvanishing element being β_{ccc}, where c coincides with the 1,4 axis of the aromatic system (see Fig. 1). The susceptibilities of Eqs. (4) and (5) are then expressed by[10,34]

$$\sqrt{I^{sp}_{pNA}}e^{i\phi^{sp}_{pNA}}=A^{1/2}\frac{N}{2}\beta_{ccc}e_z^{2\omega}F_{zyy}\langle\sin^2(\vartheta)\cos(\vartheta)\rangle e_y^\omega e_y^\omega E_\omega^2 \tag{6}$$

and

$$\sqrt{I^{pp}_{pNA}}e^{i\phi^{pp}_{pNA}}=A^{1/2}N\beta_{ccc}[e_z^{2\omega}F_{zzz}\langle\cos^3(\vartheta)\rangle e_z^\omega e_z^\omega+(\tfrac{1}{2}e_z^{2\omega}F_{zxx}e_x^\omega e_x^\omega+e_x^{2\omega}F_{xzx}e_z^\omega e_x^\omega)\langle\sin^2(\vartheta)\cos(\vartheta)\rangle]E_\omega^2, \tag{7}$$

with N as the density of the molecules on the surface and ϑ as the tilt angle of the c axis from the surface normal. The triangular brackets indicate the average over a distribution of tilt angles. In most cases a δ function of the distribution of the tilt angles is assumed.[8,22]

A β tensor with more than one nonvanishing tensor element complicates the situation. Describing pNA with two non-negligible tensor elements (β_{ccc} and β_{caa}), the form of Eqs. (6) and (7) are maintained except that all expressions of the susceptibilities in the surface coordinate system become more involved.[21] Since the general features of the results for pNA as discussed below are not critically dependent on the number of nonvanishing tensor elements, a hyperpolarizability tensor with one dominating tensor element (β_{ccc}) is assumed further on, unless stated otherwise.

The tilt angle ϑ is straightforwardly obtained by dividing Eq. (7) by Eq. (6):

$$R_P=\frac{\overbrace{2e_z^{2\omega}F_{zzz}e_z^\omega e_z^\omega cot^2(\vartheta)}^{S_{zzz}}+\overbrace{e_z^{2\omega}F_{zxx}e_x^\omega e_x^\omega}^{S_{zxx}}+\overbrace{2e_x^{2\omega}F_{xzx}e_z^\omega e_x^\omega}^{S_{xzx}}}{e_z^{2\omega}F_{zyy}e_y^\omega e_y^\omega}-\frac{\sqrt{I^{pp}_{pNA}}}{\sqrt{I^{sp}_{pNA}}}e^{i(\phi^{pp}_{pNA}-\phi^{sp}_{pNA})}. \tag{8}$$

For experiments where only the intensity of the SH signal is measured and, therefore, only the magnitude of I$_{pp}$ and I$_{sp}$ is known, Eq. (8) simplifies to

$$R_I=\left|\frac{2e_z^{2\omega}F_{zzz}e_z^\omega e_z^\omega cot^2(\vartheta)+e_z^{2\omega}F_{zxx}e_x^\omega e_x^\omega+2e_x^{2\omega}F_{xzx}e_z^\omega e_x^\omega}{e_z^{2\omega}F_{zyy}e_y^\omega e_y^\omega}\right|-\frac{\sqrt{I^{pp}_{pNA}}}{\sqrt{I^{sp}_{pNA}}}. \tag{9}$$

The tilt angle of the pNA moiety is obtained for vanishing R_I and R_P. However, there is an important difference between the solutions, as is illustrated geometrically in Fig. 2. The circle represents the ratio $\sqrt{I^{pp}_{pNA}}/\sqrt{I^{sp}_{pNA}}$ of the polarization-dependent SHG intensities, and the arrows labeled by the respective letters of Eq. (8) reflect the contributions from the different polarization combinations. The point P_0 on the circle marks the result if the phase information is retained. Neglecting for a moment a possible ϑ dependence of the F factors (see below), two of the arrows are independent of ϑ (S_{zxx}, S_{xzx}) whereas the length of the arrow containing F_{zzz} changes according to $\cot(\vartheta)^2$. As long as the sum $S_{zxx}+S_{xzx}$ ends inside the circle S_{zzz} intersects the circle at a single point only and a unique value of the tilt angle exists. In this case Eqs. (8) and (9) yield identical results, and thus phase-sensitive detection does not provide any additional information compared to intensity measurements. The situation is different if $S_{zxx}+S_{xzx}(P_1)$ ends outside the circle as shown in Fig. 2. Now S_{zzz} intersects the circle at two points and, consequently, the results are ambiguous only if intensity measurements are performed [Eq. (9)]. The correct solution requires the knowledge of the phase and, therefore Eq. (8)

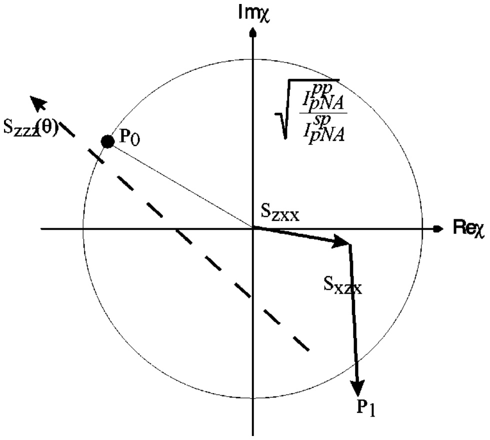

FIG. 2. Geometric illustration of Eqs. (8) and (9). For details, see text.

was to be used. The problem of ambiguous results has already addressed in Ref. 23 and 33.

Beside this crucial difference between Eqs. (8) and (9), there is another one. As inferred from Fig. 2, R_I can always become zero for a particular value of ϑ due to the elimination of the phase information and thus an apparently exact result is obtained with Eq. (9). In contrast, R_P will, in general, be complex valued for two reasons. First, the precision of measuring intensities and phases is limited. This induces a deviation of P_0 from the intersection points of $S_{zzz}(\theta)$ with the circle (Fig. 2). Second, the assumptions made in the derivation of Eq. (8) might not hold exactly, e.g., the hyperpolarizability tensor of the end group has elements additional to β_{ccc}, or the F factors are not exact descriptions of the optical properties of the system. Therefore, the extent to which R_P vanishes is an important consistency check.

C. Fresnel and local field factors

The F factors of Eqs. (4)–(9) are given by

$$F_{ijk}=F_i^{2\omega}F_j^{\omega}F_k^{\omega}L_{ii}^{2\omega}L_{jj}^{\omega}L_{kk}^{\omega}, \tag{10}$$

where the F_l^{ω}'s and $F_l^{2\omega}$ refer to the modification of the respective electric field by the presence of the interface and are expressed by the classical Fresnel factors. The L factors denote the local-field corrections.[36]

The linear optical properties of thin films on a substrate are generally described by a three-layer model (see Fig. 3), and the appropriate factors for the harmonic signal write as[18,37]

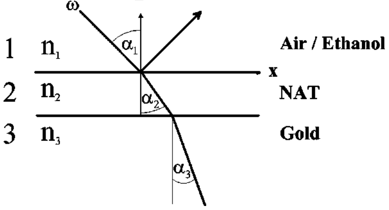

FIG. 3. Three-layer model of an organic film adsorbed on a substrate labeled by the respective indices of refraction. For clarity, only the fundamental beams are shown.

$$F_x^{2\omega}=-4\pi i\,\frac{2\omega\cos(\alpha_3^{2\omega})}{c[n_1\cos(\alpha_3^{2\omega})+n_3\cos(\alpha_1^{2\omega})]},$$

$$F_z^{2\omega}=4\pi i\left(\frac{n_3^{2\omega}}{n_2^{2\omega}}\right)^2\frac{2\omega\sin(\alpha_3^{2\omega})}{c[n_1\cos(\alpha_3^{2\omega})+n_3\cos(\alpha_1^{2\omega})]}, \tag{11}$$

$$F_y^{2\omega}=4\pi i\,\frac{2\omega}{c[n_1\cos(\alpha_1^{2\omega})+n_3\cos(\alpha_3^{2\omega})]}.$$

The factors for the fundamental field are given by

$$F_x^{\omega}=\frac{2n_1^{\omega}\cos(\alpha_1^{\omega})\cos(\alpha_3^{\omega})}{n_1^{\omega}\cos(\alpha_3^{\omega})+n_3^{\omega}\cos(\alpha_1^{\omega})},$$

$$F_z^{\omega}=-\left(\frac{n_3^{\omega}}{n_2^{\omega}}\right)^2\frac{2n_1^{\omega}\cos(\alpha_1^{\omega})\sin(\alpha_3^{\omega})}{n_1^{\omega}\cos(\alpha_3^{\omega})+n_3^{\omega}\cos(\alpha_1^{\omega})}, \tag{12}$$

$$F_y^{\omega}=\frac{2n_1^{\omega}\cos(\alpha_1^{\omega})}{n_1^{\omega}\cos(\alpha_1^{\omega})+n_3^{\omega}\cos(\alpha_3^{\omega})}.$$

The variables are defined in Fig. 3. Beside the factors describing the optical properties of stratified media, the local field acting on a molecule has to be taken into account [Eq. (10)]. In general, for adsorbates on metals local-field corrections L are due to the interaction of the E-field-induced dipole of the adsorbate with its image dipole of the metal substrate[36] and the dipole-induced dipole interaction within the molecular layer.[12,14,36] The first contribution can be safely neglected in our case. As pointed out by Ye and Shen,[36] the image dipole of an E-field-induced dipole has a negligible influence for distances of the induced dipole above the substrate beyond 2.5 Å. A SAM of NAT is about 20 Å thick, with the pNA group located on top of the layer of the hydrocarbon chains.[24] In contrast, due to the high density of the thiols with an intermolecular distance in the 5-Å range,[38] intermolecular interactions can substantially alter the external E field acting on a molecule. For a two-dimensional, crystalline array of molecules, the following correction factors expressed in the surface coordinate system were derived under the assumption of point dipoles and a uniform orientation of the dipoles:[36,39,40]

$$L_{xx}(\omega)=L_{yy}(\omega)=\left(1+\frac{\alpha_{xx}(\omega)\xi_0}{2a^3}\right)^{-1},$$

$$L_{zz}(\omega)=\left(1-\frac{\alpha_{zz}(\omega)\xi_0}{a^3}\right)^{-1}, \tag{13}$$

where ξ_0 as derived first by Topping is a constant (-9.0336).[40] α_{ll} is the linear polarizability of the molecule in the l direction of the surface coordinate system, and a is the distance between the molecules. The local-field factors affect the determination of the tilt angles in different ways. Since $L_{zz}\leqslant 1$ and $L_{xx},L_{yy}\geqslant 1$, neglection of the local-field factors yield tilt angles of the nitroaniline group which are too large compared to the real value. Furthermore, changes of the local-field factors, produce phase shifts of the SHG

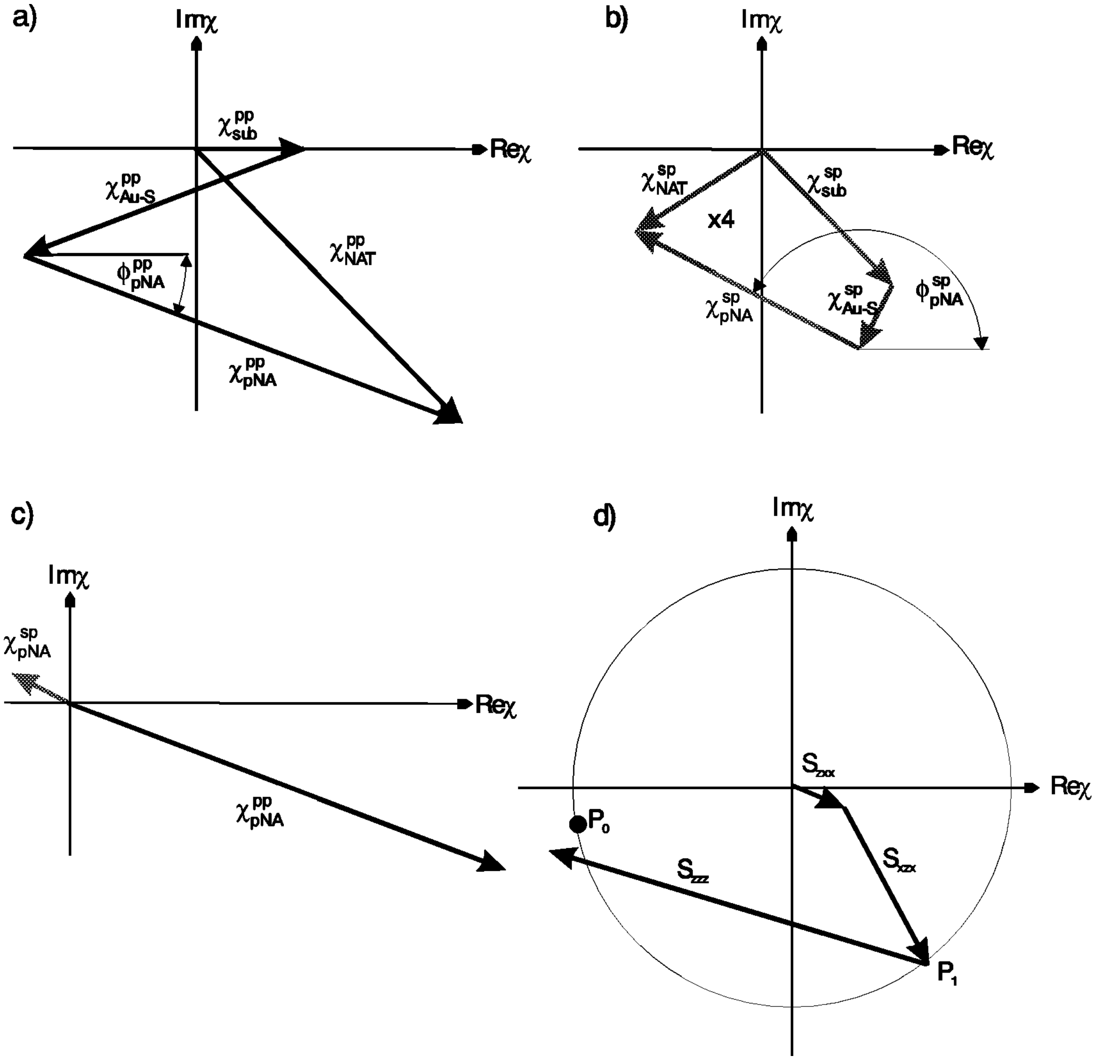

FIG. 4. Result for NAT on gold in a gaseous environment. (a) *pp* polarization. (b) *sp* polarization. (c) Relative orientation of χ^{pp}_{pNA} vs χ^{sp}_{pNA} in the complex plane. (d) Geometric illustriation of Eqs. (9) and (8) with the data for pNA. For details, see text.

signal. This is due to the Fresnel factors which are complex-valued when dealing with metal substrates. Therefore, as mentioned above, the residual value of R_P in the case of phase-sensitive detection is dependent on the values of the Fresnel and local-field factors. This represents a significant reduction in the freedom of adjusting these quantities (see Sec. V). Referring to Fig. 2, another point worth noting is that for sufficiently high polarizabilites the local fields become so strongly dependent on the tilt angle that Eq. (9) may even produce more than two solutions for ϑ.[12] Referring to Fig. 2, this is due to the fact that S_{zxx} and S_{xzx} now become ϑ dependent, as well as due to the local-field factors.

III. EXPERIMENTAL DETAILS

The synthesis of the NAT has been described elsewhere.[24] The comparative measurements with *n*-alkane thiols were performed with hexadecane thiol (Merck) or with docosane thiol synthesized by a standard procedure.[41] The purity of the substances was better than 95%. Analytical grade ethanol (J. T. Baker) was used as solvent. Gold substrates were prepared by evaporation of an approximately 100-nm-thick gold film onto a Si(100) wafer. A 5-nm-thick layer of Ti or Cr served as adhesion promoter.

The SHG experiments were performed with the samples either in contact with a N_2 or Ar atmosphere, or immersed in EtOH. A dye laser pumped by a Nd-YAG (yttrium aluminum garnet) laser (7 ns, 10 Hz) was used. The fundamental wavelengths were 700 nm for experiments in EtOH, and 635 nm for the inert gas environment.

Starting with native substrates, the intensity and phase relation of the *pp*- and *sp*-polarized SHG signals were measured. Subsequently, a complete monolayer of either NAT or an *n*-alkane thiol was adsorbed, and the measurement repeated. Phase shifts were detected by recording the interference pattern of the SHG signal from the sample, and a *y*-cut quartz reference moved along the beam path. We refer to the literature for details of phase-sensitive detection in general,[43] and at different polarizations in particular.[34] To allow phase-sensitive detection in EtOH, a liquid cell with a window parallel and in close distance to the substrate (3 mm) was used. The laser beam was incident on the sample at 45°for the gaseous environment and at 31° for the experiments in EtOH (45° onto the cell window) with respect to the surface normal.

TABLE I. Fresnel factors calculated with the linear optical constants given in Table II and Eqs. (11) and (12). The prefactors $4\pi i\omega/c$ have been omitted.

	Ex situ (635 nm)		*In situ* (700 nm)	
	Fundamental	SHG	Fundamental	SHG
x	$0.802e^{i\times 1.11}$	$0.875e^{i\times 0.47}$	$0.765e^{i\times 1.11}$	$0.931e^{i\times 0.46}$
y	$0.4145e^{i\times 1.31}$	$0.544e^{i\times 0.67}$	$0.566e^{i\times 1.27}$	$0.774e^{i\times 0.58}$
z	$1.79e^{i\times -0.41}$	$1.274e^{i\times -0.31}$	$1.82e^{i\times -0.38}$	$1.24e^{i\times -0.31}$

IV. RESULTS

A. Measurements in inert gas atmosphere

Figure 4 summarizes the results of the phase-sensitive and polarization-dependent SHG measurements. The measured susceptibilities of the NAT film and the thiol/substrate interaction are represented by Figs. 4(a) (sp-polarization) and 4(b) (pp polariziation), together with the deduced contribution of the pNA moiety. Here the phenomenological susceptibilities include Fresnel and local-field factors. The measurement in sp polarization has been oriented relative to the pp-polarized signal, which has been defined as real. The relative orientation of the polarization-dependent vectors of the pNA group depicted in Fig. 4(c) yields a ratio of

$$\frac{\sqrt{I^{pp}_{pNA}}}{\sqrt{I^{sp}_{pNA}}}e^{i(\phi^{pp}_{pNA}-\phi^{sp}_{pNA})}=7.18e^{-i170.7°}. \tag{14}$$

Figure 4(d) exemplifies the results based on Eqs. (8) and (9). For reasons detailed below, the most simple case which neglects local-field factors and equals the index of refraction of the layer with that of the environment, i.e., $n_2=1$, is assumed for the evaluation of the experimental data. The optical constants used for the data evaluation and the Fresnel factors calculated from Eqs. (11) and (12) are compiled in Tables I and II. The contributions from the zxx and xzx terms end just outside the circle given by the square root of the intensity ratio. Therefore, the arrow representing the ϑ dependence (S_{zzz}) yields an ambiguous result if the evaluation of the tilt angle is based on intensity data. Both $\vartheta=53°$ and 77° solve equation (9). This ambiguity is removed if the phase-retaining Eq. (8) is applied. A value of $\vartheta\approx 51°e^{-i3°}$ results as a solution of R_P [Eq. (9)]. Considering the inherent experimental errors the values of the tilt angles are precise within ±5°. With respect to the magnitude, the value obtained by the phase-sensitive method agrees excellently with the lower value from Eq. (9). The small residual imaginary part which is well within the precision of the phase measurements (±5°) can be taken as an indication of the quality of the measurements which relate the phase of SHG signals of different polarizations. This can be shown with calculations using slightly changed values for the relative phase between $\chi_{ads,sp}$ and $\chi_{ads,pp}$, simulating an erroneous correction of the different factors influencing the determination of the relative phases measured in different polarizations[34]. If the phase of the intensity $\sqrt{I^{sp}_{SHG}}e^{i\phi^{sp}}$ is arbitrarily changed in the range $-\pi\leqslant\phi\leqslant\pi$ relative to $\sqrt{I^{pp}_{SHG}}e^{i\phi^{pp}}$ the resulting tilt angle varies between $49°\leqslant\theta\leqslant 70°$ with imaginary parts between $-60°\leqslant\phi\leqslant 19°$.

B. Measurements in ethanol

In contrast to the inert gas environment, where a fundamental wavelength of 635 nm was used the experiments in EtOH were performed at 700 nm. The difference is due to the solvatochromic shift of the charge-transfer resonance of the pNA moiety which coincides with the second-harmonic frequency.[42] In ethanol the contribution of the pNA group was determined analogously to the experiments presented above. The ratio of the magnitude of the susceptilities amounts to

$$\frac{|\chi^{pp}_{pNA}|}{|\chi^{sp}_{pNA}|}=7.27 \tag{15}$$

from which a tilt angle of $\vartheta_{eth}\approx 36°$ results, if as in the case of the gaseous environment a two-layer model ($n_2=n_{EtOH}=1.36$) is assumed and local-field factors are neglected. The respective Fresnel factors are listed in Tables I and II. It turns out that the change of the environment to a higher index of refraction modifies the Fresnel factors in a way that the sum $S_{zxx}+S_{xzx}$ now ends inside the circle. This removes the ambiguity, and, therefore, the necessity of relating the phases of the sp- and pp-polarized signals is not required.

V. DISCUSSION

The results suggest that the p-nitro aniline end group experiences an environment-induced reorientation. However, as mentioned above, the tilt angles obtained from SHG experiments depend critically on the details of the model, i.e., the calculation of the local-field and Fresnel factors. Consequently, before discussing effects of the environment, the factors affecting the calculation of tilt angles have to be addressed together with the precision limits of such calculations due to uncertainties of the input parameters. We thus start detailing the results for the NAT-SAM in inert gas atmosphere, since in this case the results obtained by the phase-sensitive and polarization-dependent SHG experiments can be compared with those from a study combining

TABLE II. The values for the optical constants (Ref. 57).

	Ex situ (635 nm)		*In situ* (700 nm)	
	Fundamental	SHG	Fundamental	SHG
gold (n_3)	0.159+3.23 i	1.414+1.52 i	0.131+3.842 i	1.414+1.62 i
atmosphere (n_1)	1	1	—	—
ethanol (n_1)	—	—	1.36	1.374
monolayer (n_2)	1	1	1.36	1.374

IR and NEXAFS.[24] With these linear techniques a tilt angle of $\vartheta = 52°$ for the 1,4 axis of pNA was found. As indicated in Sec. IV, we have to neglect the local-field factors (LFF's) and adopt a two-layer model, in order to achieve agreement between the linear spectroscopies and SHG. Otherwise, the SHG experiments yield deviations to much smaller tilt angles. This is rather unexpected in view of the models usually applied to describe the optical properties of ultrathin organic films. Before discussing possible reasons for this finding, we first detail why the value obtained by the linear techniques is considered a reliable reference value.

NEXAFS can be safely excluded to be a source of error. The dipole moment of the electronic transition probed has a well-defined direction,[24] thus introducing no principle uncertainties in the tilt angle determination. In contrast, IR reflection (IRRAS) has to rely on certain assumptions which can sensitively affect the results. Determining molecular orientation by IRRAS relies on the comparability of the IR transition dipole moments in bulk material and thin films. This assumption does not hold necessarily, particularly in the case of NAT where the pNA group is located right at the interface where the environment can be rather different from the bulk. However, despite this uncertainty, for two reasons we believe that IRRAS reflection is not the cause of the discrepancy. First, the ratio of band intensities of the sym- and asym-NO_2 vibration from which the orientation was deduced has to be changed beyond the experimental uncertainty to produce a tilt angle compatible with the interpretation of the SHG data, which take into account LFF's and/or a three-layer model. Second, the lack of the N-H vibration in the IRRAS spectrum, which indicates an orientation parallel to the metal surface, is in excellent agreement with the orientation of the pNA ring, as determined by IRRAS and NEXAFS.[24]

We now turn to a discussion of the local-field factors. As already pointed out, the electric field acting on the pNA group is strongly dependent on the LFF's and, therefore, the interpretation of SHG experiments is sensitively dependent on their choice. Unfortunately, the literature does not provide a conclusive picture. Partly, local-field effects are taken into account according to Eq. (13) (Refs. 12–15) or the somewhat simpler Lorentz form is used.[16,17] Other works completely neglect a possible influence of LFF's.[22,21,44] Also the necessity to take local-field factors into account is ambiguous in the literature. For the systems investigated in Refs. 22 and 12 the effect of local-field factors on the tilt angle determination is shown to be negligible, whereas McGilp, Tang, and Cavanagh demonstrated a shift of the molecular tilt angle by approximately 20° to a more upright orientation due to local-field corrections.[14] By taking local-field factors into account, additional parameters such as the polarizability tensor and the intermolecular distance are introduced. Since these quantities are usually known within certain limits only, a considerable uncertainty in the determination of tilt angles can result as now demonstrated. For pNA the linear and nonlinear polarizability tensors $\boldsymbol{\alpha}$ and $\boldsymbol{\chi}$ are rather well known since pNA has been one of the systems in nonlinear optics investigated intensively both experimentally and theoretically.[11,45,46] The linear polarizability of the pNA moiety has its largest component along the molecular axis [$\alpha_{cc}^{\omega} = 21$ Å^3 (Refs. 45 and 46)] although the polarizability along the a axis is also considerable ($\alpha_{aa}^{\omega} = 0.66\alpha_{cc}^{\omega}$). Compared to these nonresonant values, the polarizability at the harmonic wavelength is estimated to be increased by approximately 30%, i.e., $\alpha_{aa}^{\omega} = 16.4$ Å^3 and $\alpha_{cc}^{\omega} = 27.3$ Å^3).[45] The nonlinear polarizability tensor $\boldsymbol{\chi}$ is instead dominated by the element β_{ccc} along the 1,4 axis, which in our calculations is set to unity. The next important tensor element is $\beta_{caa} \leqslant \frac{1}{6}\beta_{ccc}$.[45,46] With the known average intermolecular distance a in the range of $5 \leqslant a \leqslant 5.5$ Å, which is deduced from the NAT coverage,[24] basically all input parameters are known. To gain more insight into how much the interpretation of SHG data is influenced by the local-field factors, different parameters such as the tilt ϑ and twist angle ψ, the respective distribution widths $\Delta\vartheta$ and $\Delta\psi$, and the intermolecular distance a are varied. The above given values for the two components of the linear polarizability are taken for the calculations, and in the treatment of the two-non-negligible tensor elements of the SHG susceptibility tensor we follow Refs. 21 and 47 which leads to a modification of Eqs. (6) and(7).

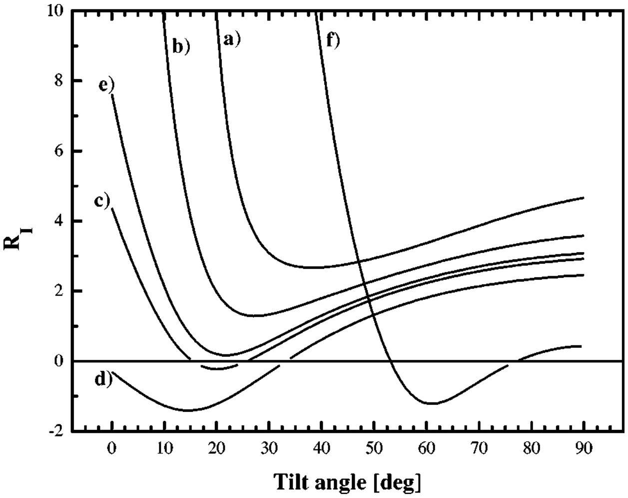

FIG. 5. Effect of local-field factors and the variation of the twist angles ψ of the pNA group on the calculation of tilt angles from Eq. (9). Tilt angles are given by $R_I = 0$. The intermolecular distance is set to 5 Å (a) $\psi = 0°$. (b) $\psi = 32°$. (c) $\psi = 50°$. (d) $\psi = 70°$. (e) Isotropic distribution of ψ. (f) Local-field factors neglected.

Essentially, due to the two components of the linear polarizability, the twist angle ψ of the pNA group becomes a parameter that has a strong influence on the solution of Eq. (9). In Fig. 5 the solution of Eq. (9), generalized to two nonvanishing tensor elements of the molecular hyperpolarizability, is shown for a selection of twist angles ψ, where ψ is defined such that for $\psi = 0°$ the pNA ring plane is perpendicular to the plane spanned by the molecular 1,4 axis and the s-polarization direction. The tilt angles are given by the intersection of the curves with the line at $R_I = 0$. These calculations assume a distance of $a = 5$ Å between the pNA groups; the distance found for a complete monolayer of n-alkane thiols[25]. Postponing the discussion of how the width of the angular distribution affects the calculation we assumed Gaussian distributions for ψ and ϑ. In the calculations presented in Fig. 5 the halfwidths were fixed to $\Delta\psi = 10°$ and $\Delta\vartheta = 15°$. These widths for the angular distributions are based on an estimation from the vanishing intensity of the N-H vibration in IRRAS and the precision of the orientation of the π'-transition from NEXAFS[24]. Additionally, the result for an isotropic distribution of the twist angle ψ is shown. For comparison the curve neglecting the local fields is included as well. The same Fresnel factors as in Sec. IV were used. Inspection of Fig. 5 shows three aspects. Firstly, the tilt angle is strongly dependent on the twist angle. Large twist angles, i.e. $\psi \geqslant 75°$ yield a unique solution with values around 30° whereas for $\psi \approx 50°$ ambiguous solutions are obtained. For even lower values the curves no longer intersect the zero line, i.e. no solution for the tilt angle exists. This holds as well for the isotropic case. Second, even though there is quite a bit of variation in the tilt angle the values are always considerably lower compared to the curve neglecting the local-field factors. This means that local-field factors, based on the literature data for the polarizability, change the calculated tilt of the 1,4 axis by at least 20°, depending on the exact value of the twist angle. Third, comparison of these calculations with the results from the linear spectroscopies reveals a discrepancy. From NEXAFS/IR investigations, a twist angle of 32° was found,[24] i.e., a value where no solution for ϑ exists according to Fig. 5.

The strong variation of ϑ as a function of ψ is caused by the tensor of the linear polarizability. Neglecting local-field factors, the influence of ψ is solely dependent on the second-order susceptibility. Since the molecular hyperpolarizability β is dominated by β_{ccc}, the effect of ψ on the tilt angle is weak and cannot explain the differences between SHG and NEXAFS/IR. Taking the literature values for β, i.e., $\beta_{ccc}/\beta_{caa} \geqslant 6$,[45] results in a variation of the tilt angle between 50°and 56°, and for the twist angle found by NEXAFS and IRRAS (ψ=32°) ϑ equals 54°, in excellent agreement with the value found by linear spectroscopies.

The calculation of Fig. 5 assumed an intermolecular distance of 5 Å. However, as estimated from x-ray photoemission spectroscopy data[24] and SHG adsorption studies,[48] the lower limit for the saturation coverage θ of an NAT monolayer is 80% of a SAM of *n*-alkane thiols. Even though this increases the average intermolecular distance a to $\approx$5.5 Å, the discrepancy to the NEXAFS/IR data is not removed. Only the tilt angles shift by about 10° towards a more canted orientation of the pNA group. In order to achieve agreement between IR/NEXAFS and SHG for both twist and tilt angles, the average intermolecular distance a has to be increased to 7 Å. At this distance the local-field correction factors deviate from 1 by less than 20%. However, $a = 7$ Å corresponds to a coverage of $\theta \approx 50\%$ which is incompatible with XPS and SHG adsorption experiments.[24,48] Another point to be considered is the distribution width of the angles. Compared to the curve of Fig. 5(f), which neglects local-field factors and assumes a well-defined tilt angle, the other curves are calculated using tilt angle distributions $\Delta\vartheta$ and $\Delta\psi$. The former has the effect that an increase in the angular width shifts the obtained result to more canted orientations, since more upright molecules contribute more than the more canted. As mentioned above, the width adopted in the calculation of Fig. 5 is the broadest width that may be compatible with the IR results.[24] If a strongly peaked distribution is assumed, agreement between NEXAFS and SHG with inclusion of local-field corrections is only achievable for intermolecular distances exceeding 9 Å ($\theta \approx 0.3$). For this distance the correction induced by the local-field factors is less than 10% and, therefore, becomes negligible. Broadening of the angular distribution thus compensates for the effect of the local field on the calculation of tilt angles.

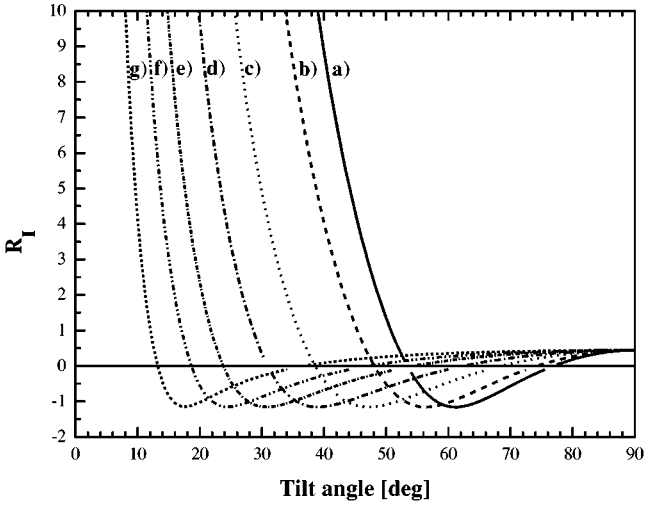

FIG. 6. Tilt angle dependence as a function of the index of refraction of the molecular layer. (a) $n = 1$, (b) $n = 1.1$, (c) $n = 1.3$, (d) $n = 1.5$, (e) $n = 1.75$, (f) $n = 2$, and (g) $n = 2.4$ for the fundamental and harmonic radiation. The imaginary part of the index of refraction is 0 in either case.

Besides the problem of defining the correct local-field factor, which only becomes apparent by comparing SHG with other techniques, the question of which Fresnel factors to use turns out to be nontrivial. In linear optics such as ellipsometry, IR spectroscopy or surface-plasmon spectroscopy the optical properties of a monolayer are modeled by three layers and values for the index of refraction of the layer typical for organic materials produce satisfying results.[49–51] For SHG, in contrast, the situation is not clear. This was already addressed by Zhang, Zhang, and Wong[23], who pointed out that the implicit assumptions of the model suggested by Mizrahi and Sipe[52] are difficult to justify. Zhang, Zhang, and Wong based the evaluation of their SHG data on a three layer model as did other authors.[14,16,13,18–20] But two layer models, in which only the indices of refraction of the surrounding media are considered, were applied as well.[21,22] Zhang, Zhang, and Wong calculated variations of the tilt angles by more than 30°if the index of refraction of the organic layer is varied between the values of the environment and the bulk of the substrate.[23] For the system presented here agreement between the tilt angle determined with SHG and NEXAFS/IR is only obtained if an index of refraction of $1 \leqslant n \leqslant 1.1$ is used for the monolayer (local-field factors still neglected). Since, in general, the dielectric constant of the monolayer only modifies the Fresnel factor of the component perpendicular to the surface, an increasing n_2 decreases the respective electric-field strength. Therefore, the resulting molecular tilt angle changes to lower values. This can be seen in Fig. 6, where R_I is plotted against the refractive index of the monolayer. Only the real part of the refractive index is varied, since the influence of an imaginary part deviating from zero is mainly a vertical upward shift of the R_I curves in Fig. 6, and therefore of only minor importance for this discussion. The tilt angles are given by the intersection of the curves with the zero line. For the calculation, a fundamental wavelength of 635 nm, was assumed and the Fresnel factors were determined according to Eqs. (11) and (12). For the reasons outlined above, the results are ambiguous. Only for $n_2 \approx n_1 = 1$ do the tilt angles agree with the results from NEXAFS/IR. From the calculation one could conclude as well that for $n_2 = 1.75$ the more canted orientation of $\vartheta \approx 53°$ might be the correct solution. However, this can be ruled out, since this solution is excluded by a phase-sensitive evaluation based on Eq. (8). Figure 6 shows that an increase of the refractive index n_2 shifts the tilt angle into the same direction as local-field factors, i.e., to lower values. There is no way to achieve agreement with the NEXAFS/IR data using the three-layer model for the calculation of the Fresnel factors. Thus our results support the two-layer model used in Refs. 21 and 52. However, the precise value of the refractive indices used for the gold substrate are of only minor importance. Deviations of 10% compared to the values given in Table I are found in the literature. These differencies result in a shift of the respective curves in Fig. 6 by less than 4° to a more canted orientation.

The applicability of the two-layer model for orientational analysis with nonlinear optical techniques is further supported by IR-*vis*-sum-frequency generation experiments. In these experiments the application of the two-layer model again leads to very good agreement with literature values for the orientation of *n*-alkane thiols.[53,54]

Closing the discussion of the second-harmonic generation from a NAT-SAM in an inert gas atmosphere, we address possible reasons why the simple models fail. One crucial point is the model the calculation of LFF's is based on. First, it assumes a crystalline structure of the SHG active units, i.e., a uniform orientation. Releasing this rigid geometry alters the results. Cnossen, Drabe, and Wiersma extended the calculation of local-field effects to disordered systems, and found deviations compared to the crystal model.[12] However, the magnitude of this change is dependent on the details of the system, e.g., the tilt angle of the molecule and polarizability, and, therefore, it is difficult to estimate the importance of this effect for our system. At present we can neither support nor disprove the correctness of an ordered structure, since no microscopic information about the lateral arrangement of the *p*NA units is available. The second point is the validity of the assumption of a point source dipole model. Since the dimension of the *p*NA unit is comparable to the intermolecular distance, this assumption is unlikely to hold. Again, the importance of this effect is strongly dependent on the details of the system, particularly the orientation of the molecules relative to each other. The third point is the question of the validity of the electric dipole approximation. Linear optics averages over the whole thickness of the organic layer, and, thus, a representation by an own index of refraction seems justified. In contrast, generation of a second-harmonic signal can be very local. Since in the present case the SHG-active *p*NA group is located at the outermost region of the NAT layer, where the optical properties change within a very short distance, this ansatz might be questioned. The field perpendicular to the surface exhibits a gradient within the dimension of the *p*NA moiety, and thus higher-order contributions might come into play.[55]

We now turn to a comparison of the results for different environments. A crucial point is how safely the phenomenological model for a SAM of NAT in a gaseous environment (a two-layer model with indices of refraction given in Table II, with a LFF equal to 1) derived from the comparison of results from linear spectrocopies, and SHG can be transferred to the EtOH environment. If the correct model for the gaseous environment were local-field factors deviating from one and three layers rather than two, the factors just discussed must affect the signals in a way that the phenomenological model results. All these mentioned factors which could account for the deviation from the ''standard'' model (three-layer model, the LFF not always equal to 1) should become less important in solution. The indices of refraction of the film and the ambient medium are very similar, thus reducing the influence of field gradients. The effect of local fields should be reduced as well, due to the presence of the dielectric medium. As a result, including local-field factors and/or assuming three layers causes the tilt angle to shift to smaller values than the phenomenological model. Since no simple theory exists to estimate the magnitude of these effects, we cannot give a precise value for the environment induced reorientation of the *p*NA group. Instead we are limited to the calculation of an upper limit. For NAT in contact with EtOH, this value is $\vartheta = 36°$, i.e., the minimum change of the tilt angle is about 16°.

An environment-induced reorientation of a related substance [nitrobenzoic acid (NBA)] adsorbed on silica surfaces was found previously in Ref. 22. The authors also observed a more upright orientation of NBA in the solvent, and assigned this to a weakened interaction of the nitrogroup with the substrate in the presence of the solution. The present case is different since the *p*NA group of NAT is separated from the substrate by the alkyl spacer layer by more than 10 Å. Instead, we ascribe the reorientation to the wetting of the nitroaniline groups by the polar solvent ethanol. This wetting induces an attenuation of the dipole-dipole interaction between the *p*NA groups of the order of the static dielectric constant of ethanol (from $\epsilon = 1$ to $\epsilon_{ethanol} = 21$).[56] The interaction energy of the van der Waals forces between the adsorbed NAT molecules is increased, instead.[56] The resulting pNA orientation in the solvent is therefore the result of an optimization of the different energy contributions of the wetting by the solvent, the reduced dipole-dipole interaction, and the stronger van der Waals interactions. Since the methylene chains of NAT are relatively disordered, a penetration of the solvent into the layer to some extent is likely, in contrast to earlier findings for alkane thiols.[58,59]

The interpretation of an environment driven reorientation is not unique, since a change of the distribution of the tilt angle can, in principle, produce the same effect. Assuming a change from a δ to a Gaussian distribution, an apparent reorientation by 16° is assumed by increasing the spread of the tilt angle to a half-width of $\Delta\vartheta = 60°$. That immersion in EtOH induces such a high degree of disorder is hard to believe, even though we cannot decide at present whether reorientation or disordering prevails. Reorientation vs disordering can, in principle, be decided by comparing the signal intensities of *p*NA in both environments. However, for NAT this possibility is complicated by the fact that *p*NA exhibits a pronounced solvatochromic behavior, with β_{ccc} being dependent on the environment.

VI. CONCLUSION

The orientation of the *p*-nitroaniline moiety of 12-(4-nitroanilino)-dodecane thiol adsorbed on gold was studied by SHG in an inert gas environment, and in contact with ethanol. Compared to molecular adsorbates studied with SHG, so far NAT on gold represents a more complicated system. The measured signal is a superposition of three contributions, i.e., from the metal substrate, the thiol-substrate interaction, and the *p*NA group, which are comparable in magnitude. Separation of the signal from the *p*NA group requires a knowledge of the interaction term. That is determined by a comparison with unsubstituted *n*-alkane thiols. Since for metal substrates the different contributions are phase shifted relative to each other, phase-sensitive measurements are required to determine the contribution of the *p*NA moiety. The system studied here represents an example where intensity measurements in *sp* and *pp* polarizations produce ambiguous results. Knowledge of the phase relation between the different tensor elements of the susceptibility of the *p*NA group is mandatory.

The value of the tilt angle is sensitively dependent on the model applied for the an evaluation of the SHG. A detailed discussion of the different critical factors such as the local fields, Fresnel factors, and linear and nonlinear polarizabilities reveals that SHG can become a very inaccurate method if certain input parameters lack precision. Again, the phase information proved to be invaluable for choosing among different possibilites. A persisting problem is the question of the correct local fields and proper Fresnel factors. In the present case we adopted a phenomenological approach by comparing the results of the SHG experiments with those from other techniques. For a monolayer in a gaseous environment, a two-layer model and ignoring local-field corrections yields excellent agreement between the SHG experiments and the results from NEXAFS and IR spectroscopy.[24]

Based on the phenomenological model we found a reorientation of the *p*NA group upon a change of the environment from an inert gas to liquid ethanol. This reorientation from 52° to at least 36° is assigned to the change in the relative importance of van der Waals and dipole-dipole interactions between NAT molecules, and between the contact of the NAT with the solvent.

ACKNOWLEDGMENTS

The authors are indebted to M. Grunze for his continuous support. We would like to thank J. J. Wolff for synthesizing the *p*-nitroaniline thiol and J. Dennis at the University of Washington for helpful discussions. Support by the Deutsche Forschungsgemeinschaft (Bu820/10-1) and Fonds der Chemischen Industrie is gratefully acknowledged.

---

*Present address: Department of Bioengineering, University of Washington, P.O. Box 357962, Seattle, WA 98195.

[1] A. Ulman, *Ultrathin Organic Films* (Academic, Boston, 1991).

[2] T. Hui Ong, P.B. Davies, and C.D. Bain, Langmuir **9**, 1836 (1993).

[3] M.A. Hines, J.A. Todd, and P. Guyot-Sionnest, Langmuir **11**, 493 (1995).

[4] C.D. Bain, J. Chem. Soc., Faraday Trans. **91**, 1281 (1995).

[5] M. Buck, F. Eisert, J. Fischer, M. Grunze, and F. Träger, Appl. Phys. A: Solids Surf. **53**, 552 (1991).

[6] M. Buck, O. Dannenberger, and J.J. Wolf, Thin Solid Films **284**, 396 (1996).

[7] V. Vogel and Y.R. Shen, Annu. Rev. Mater. Sci. **21**, 515 (1991).

[8] R.M. Corn and D.A. Higgins, Chem. Rev. **94**, 107 (1994).

[9] Y.R. Shen, Surf. Sci. **299/300**, 551 (1994).

[10] Y.R. Shen in *Molecular Nonlinear Optics*, edited by J. Zyss (Academic, San Diego, 1994), p. 101.

[11] *Nonlinear Optical Properties of Organic Molecules and Crystals*, edited by D.S. Chemla and J. Zyss (Academic, Orlando, 1987).

[12] G. Cnossen, K.E. Drabe, and D.A. Wiersma, J. Chem. Phys. **97**, 4512 (1992).

[13] L.M. Hayden, Phys. Rev. B **38**, 3718 (1988).

[14] J.F. McGilp, Z.-R. Tang, and M. Cavanagh, Synth. Met. **61**, 181 (1993).

[15] T. Rasing, Y.R. Shen, M.W. Kim, and S. Grubb, Phys. Rev. Lett. **55**, 2903 (1985).

[16] H. Hsiung, G.R. Meredith, H. Vanherzeele, R. Popovitz-Biro, E. Shavit, and M. Lahav, Chem. Phys. **164**, 539 (1989).

[17] N. Bloembergen, *Nonlinear Optics* (Benjamin, New York, 1965), p. 69.

[18] C. Hirose, N. Akamatsu, and K. Domen, Appl. Spectrosc. **46**, 1051 (1992). In this work, Fresnel factors based on Ref. 37 are derived, but in the formula given for the fundamental radiation the factor $(n_3^{\omega}/n_2^{\omega})^2$ has to be additionally included. An additional sign takes account of the different conventions for the coordinates choosen in this reference compared to our work.

[19] E.A. Potterton and C.D. Bain, J. Electroanal. Chem. **409**, 109 (1996).

[20] M. Buck, Ch. Dressler, M. Grunze, and F. Träger, J. Adhes. **58**, 227 (1996).

[21] D.J. Campbell, D.A. Higgins, and R.M. Corn, J. Phys. Chem. **94**, 3681 (1990).

[22] T.F. Heinz, H.W.K. Tom, and Y.R. Shen, Phys. Rev. A **28**, 1883 (1983).

[23] T.G. Zhang, C.H. Zhang, and G.K. Wong, J. Opt. Soc. Am. B **7**, 902 (1990).

[24] A. Wesch, O. Dannenberger, J.J. Wolf, Ch. Wöll, and M. Buck, Langmuir **12**, 5330 (1996).

[25] L.H. Dubois, R.G. Nuzzo, Annu. Rev. Phys. Chem. **43**, 437 (1992).

[26] M. Grunze, Phys. Scr. B **T49**, 711 (1993).

[27] A. Ulman, Chem. Rev. **96**, 1533 (1996).

[28] D.R. Jung and A.W. Czanderna Crit. Rev. Solid State Mater. Sci. **19**, 1 (1994).

[29] H.O. Finklea, J. Electroanal. Chem. **19**, 105 (1996).

[30] Th. Wink, S.J. Van Zuilen, A. Bult, and W.P. van Bennekom, Analyst (Cambridge, U.K.) **122**, 43R (1997).

[31] B. Vökel, A. Gölzhäuser, H.U. Müller, C. David, and M. Grunze, J. Vac. Sci. Technol. B **15**, 2877 (1997).

[32] M. Buck, F. Eisert, J. Fischer, F. Träger, and M. Grunze, J. Vac. Sci. Technol. A **10**, 926 (1992).

[33] B.U. Felderhof, A. Bratz, G. Marowski, O. Roders, and F. Sieverdes, J. Opt. Soc. Am. B **10**, 1824 (1993).

[34] M. Buck, F. Eisert, M. Grunze, and F. Träger, Appl. Phys. A: Solids Surf. **60**, 1 (1995).

[35] R. Kohring (unpublished).

[36] P. Ye and Y.R. Shen, Phys. Rev. B **28**, 4288 (1983).
[37] W.N. Hansen, J. Opt. Soc. Am. **58**, 380 (1968).
[38] N. Camillone III, T.Y.B. Leung, and G. Scoles, Surf. Sci. **373**, 333 (1997).
[39] A. Bagchi, R.G. Barrera, and B.B. Dasgupta, Phys. Rev. Lett. **44**, 1475 (1980).
[40] J. Topping, Proc. R. Soc. London, Ser. A **114**, 67 (1927).
[41] O. Dannenberger, diploma thesis, Heidelberg, 1993.
[42] G. Berkovic and E. Shvartsberg, Appl. Phys. B: Photophys. Laser Chem. **53**, 333 (1991).
[43] M. Stähelin, D.M. Burland, and J.E. Rice, Chem. Phys. Lett. **191**, 245 (1992).
[44] G. Marowsky, G. Lüpke, R. Steinhoff, L.F. Chi, and D. Möbius, Phys. Rev. B **41**, 4480 (1990).
[45] K.V. Mikkelsen, Y. Luo, H. Ågren, and P. Jorgensen, J. Chem. Phys. **100**, 8240 (1994).
[46] S.H. Karna and P.N. Prasad, J. Chem. Phys. **94**, 1171 (1991).
[47] B. Dick, Chem. Phys. **96**, 199 (1985).
[48] O. Dannenberger, Ph.D. thesis, University of Heidelberg, 1996.
[49] M. Born and E. Wolf, *Optics* (Springer-Verlag, Heidelberg, 1975).
[50] H. Raether *Surface Plasmons*, Springer Tracts in Modern Physics Vol. 111 (Springer-Verlag, Heidelberg, 1989).
[51] P. Laibinis, G.M. Whitesides, D.L. Allara, and Y.-T. Tao, A.N. Parikh, R. G. Nuzzo, J. Am. Chem. Soc. **109**, 2358 (1991).
[52] V. Mizrahi and J.E. Sipe, J. Opt. Soc. Am. B **5**, 660 (1988).
[53] A. Lampert, M. Buck, F. Eisert, and M. Grunze (unpublished).
[54] M. Himmelhaus, M. Buck, F. Eisert, and M. Grunze (unpublished).
[55] P. Guyot−Sionnest, W. Chen, and Y.R. Shen, Phys. Rev. B **33**, 8254 (1986).
[56] J. Israelachvili, *Intermolecular and Surface Forces* (Academic, London, 1992).
[57] G. Hass and C. Hadley, in *American Institute of Physics Handbook* (McGraw Hill, New York, 1982)
[58] S.M. Stole and M.D. Porter, Langmuir **6**, 1199 (1990).
[59] C.J. Sandroff, S. Garoff, and K.P. Leung, Chem. Phys. Lett. **96**, 547 (1983).